RSC Advances

ROYAL SOCIETY OF CHEMISTRY

www.rsc.org/advances

Modifying the Carbon Fiber-Epoxy Matrix Interphase with Silicon Dioxide Nanoparticles

Wenzhen Qin[1, 2], Frederic Vautard[2], Per Askeland[2], Junrong Yu[1 *] and Lawrence Drzal[2, 3 *]

[1]State Key Laboratory for Modification of Chemical Fibers and Polymer Materials, College of Materials Science and Engineering, Donghua University, Shanghai 201620, China

[2]Composite Materials and Structures Center, Michigan State University, East Lansing, Michigan 48824, USA

[3]Chemical Engineering and Materials Science Department, Michigan State University, East Lansing, Michigan 48824, USA

*Corresponding authors:

E-mail:yjr@dhu.edu.cn (J. R. Yu), Tel: +86 21 6779 2945,

drzal@egr.msu.edu (L. T. Drzal), Tel: +1 517 353 5466,

Abstract :

Nanoparticle modification of the carbon fiber-epoxy interface was investigated by depositing silicon dioxide (SiO_2) nanoparticles on the surface of carbon fibers (CFs) using a conventional sizing process by immersing CFs tows in a SiO_2 nanoparticle suspension. The surface density of the nanoparticles and the uniformity of their dispersion were characterized by scanning electron microscopy. CF/epoxy composites were fabricated to study the effect of the SiO_2 nanoparticle coating on the CF/epoxy composite interfacial properties. Interfacial adhesion was assessed by measuring the interfacial shear strength (IFSS) with the single fiber fragmentation test. A 44 % improvement of the IFSS was obtained with a SiO_2 relative concentration of 1.3 wt. %, compared with non-coated CFs. This increase was the result of an increase of the shear modulus of the matrix in the interphase region caused by the presence of the SiO_2 nanoparticles. Coating CFs with SiO_2 nanoparticles has been shown to be a simple, scalable, and cost effective method to increase the

interfacial mechanical properties in CF/epoxy composites.

Keywords:

Polymer matrix composites (PMCs), carbon fibers, coating, nanoparticles, fiber/matrix bond

1. Introduction:

Due to their outstanding mechanical properties and low density, the interest in using for carbon fiber reinforced polymer composites (CFRPs) keeps growing. The main markets are aerospace, aeronautics, wind energy, construction, automotive, sport and recreation[1] . It is now well established that for a specific fiber reinforcement and polymer matrix system, the interfacial properties and particularly the interfacial adhesion between the fiber and the matrix is an important factor and can have a substantial effect on the ultimate performance of the composite[2-4]. This is due to the formation of an interphase region in the matrix close to the surface of the fibers where the matrix properties are different from the properties of the bulk, resulting from specific interactions between some the constituents of the matrix and the fiber surface[5, 6]. An 'engineered' interphase can enhance the structural integrity of the composite and lead to better transfer of the stress between the matrix and the fibers [7]. In order to increase the level of interactions between the matrix and the fiber surface and to remove weak boundary layers of carbon generated after the carbonization step, CFs are surface treated. Numerous approaches for CF surface treatment have been studied, such as electro-chemical oxidation [8], oxidation in strong acids [9], thermo-chemical oxidation [10], UV-ozone [11], plasma treatment in various gazes [12-14], and plasma polymerization [15, 16]. After surface treatment, commercial CFs are often sized, *i.e.* their surface is covered with a layer of resin (usually epoxy monomers), which protect the fibers from damage during handling and composite manufacturing. This sizing generates an interphase in the composite, as it can partially dissolve in the matrix, and as some constituents of

the matrix can also diffuse into it, generating a gradient in concentration of those constituents (and consequently a gradient in mechanical properties) from the bulk to the fiber surface. Therefore, the composition of the sizing has a great influence on the level of interfacial adhesion and the level of the mechanical properties of the composites [17-19].

Recently nanoparticles have attracted attention due to their mechanical properties and reinforcement potential, because of their high surface/volume ratio [20]. It has been demonstrated that the incorporation of carbon nanotubes [21], graphene nanoplatelets [22-24] and titanium oxide nanoparticles [25] in the sizing could increase the adhesion strength between the fiber and the matrix.

Silicon dioxide (SiO_2) nanoparticles are high surface area spherical particles that have a high density of surface silanol groups, which makes them a valuable candidate to generate strong interactions (covalent bond) with an epoxy sizing [26, 27]. Moreover, SiO_2 nanoparticles are cost-effective and safe [28]. Liu *et al.*[29] reported that an improvement of interfacial adhesion, quantified by the interfacial shear strength (IFSS) measured with the single fiber fragmentation test, could be obtained by adding silica nanoparticles to an epoxy matrix with a volume concentration as low as 2 vol. % (increase of the IFSS from 34 to 44 MPa). Hsieh *et al.* [30]showed that the incorporation of silica nanoparticles in an epoxy matrix increased its fracture toughness and the fracture toughness of the corresponding CF composite. Nevertheless, the adding of silica nanoparticles in an epoxy matrix may result in an increase in viscosity, making the manufacture of a fiber reinforced composite by liquid molding methods more difficult. Furthermore the nanoparticles can be 'filtered' by the fiber tows resulting in their non-uniform distribution throughout the composite part. Incorporation of silica nanoparticles in the fiber sizing eliminates these issues by placing the nanoparticles in the interphase where they function to increase the mechanical properties by an enhancement of the mechanical

properties of the interphase region.

In this investigation, a simple coating process was developed. CFs were immersed into a SiO_2 nanoparticle suspension to coat their surface with a nanoparticle layer. This can be considered as the batch process equivalent to a continuous fiber sizing process, which enables a straightforward scale-up compatible with current industrial practice. (3-Aminopropyl) triethoxysilane (APTES) was grafted at the surface of the particles in order to obtain a high surface density of particles with good dispersion and also to improve the level of interactions with the epoxide functional groups of the matrix (generation of covalent bonding). The influence of the surface density in SiO_2 nanoparticles and of the quality of their dispersion on the interfacial properties was quantified by measuring the IFSS, which was carried out with a single fiber fragmentation test. A significant improvement of the adhesion strength was obtained with optimal conditions.

2. Materials and methods

2.1. Materials

The silicon dioxide (SiO_2) nanoparticles used in this study were purchased from Sigma-Aldrich. Their average surface area is around 395 m^2*g^{-1} and their diameter is about 7 nm, but aggregates of particles were obviously present. (3-Aminopropyl) triethoxysilane (APTES) was also obtained from Sigma-Aldrich.

Polyacrylonitrile (PAN)-based CFs AS4 (12K) supplied by Hexcel Co. were used in this study. The fibers were surface treated but not sized. Their diameter was about 7.1 μm. Before the dip-coating process, the fibers were first surface treated with a UV/ozone oxidation treatment developed in our laboratory. In comparison to the commercial surface treatment, the UV/ozone oxidation surface treatment generates a higher content with advantageous functional groups

(hydroxyl groups and carboxylic acids). More information about the CF surface properties generated by this technology can be found elsewhere [11, 31].

Epoxy resin Epon 828 was supplied by Hexion Specialty Chemicals. The curing agent was m-phenylenediamine (mPDA) and was purchased from Sigma-Aldrich. 1-Methyl-2-pyrrolidinone (NMP) was chosen as the solvent for the coating solution and was provided by VWR International. All chemicals were used as received.

2.2. Experimental Method

2.2.1. Grafting of APTES on SiO_2 nanoparticles

The SiO_2 nanoparticles were first heated under vacuum at 60 ºC for 2 h and then dispersed in ethanol at 60 ºC for 30 min with constant stirring (the weight ratio of SiO_2 and ethanol was 1:20). APTES was slowly added into the SiO_2/ethanol suspension (the weight ratio of SiO_2 and APTES was 5:1). The mixture was constantly stirred and maintained at 60 ºC for 2 h in a glass beaker covered with aluminum foil. The foil was then removed and the ethanol was evaporated. The particles were further dried under vacuum at 60 ºC overnight. The obtained material was designated APTES-SiO_2.

2.2.2. Preparation of APTES-SiO_2 coated CFs and epoxy-only coated CFs

The procedure used for coating CFs with APTES-SiO_2 particles is described in Figure 1. First, Epon 828 was dissolved in NMP at a concentration of 1 wt %. APTES-SiO_2 particles were added to the solution at concentrations of 0.5, 1, 2 and 3 wt % and were dispersed by sonication (Cole-Parmer's horn sonication device 750-Watt Ultrasonic Homogenizer) at 200 W output power, for 1.5 h, with continuous stirring. CFs tows were dipped into the APTES-SiO_2 suspensions for 10 sec and slowly pulled out. Subsequently, the fibers were dried in vertically an oven at 70 ºC for 3 h. The coated CFs were designated as APTES-SiO_2 coated CFs. For epoxy-only coated CFs, 1 wt% Epon 828 was

dissolved in NMP, and CFs were dipped into epoxy solution for 10 sec. Then the coated CFs were dried according to the same process used with the APTES-SiO_2 coated CFs

2.2.3. Single fiber fragmentation test coupons

A single CF was placed at the center of a dog bone-shaped cavity in a silicone mold. The fibers were kept straight by applying rubber cement to each end. A freshly made Epon 828-mPDA mix (mPDA at a concentration of 14.5 phr) and the silicone mold with the single fiber were degassed under vacuum at 75 ºC. Then, the epoxy mix was poured into the mold, covering the fiber completely. The composite was cured at 75 ºC for 2 h and post-cured at 125 ºC for 2 h. The cured specimens were sanded with paper of increasing grit size and then polished with a Struers Abramin machine until they were transparent and perfectly flat.

2.3. Characterization methods

2.3.1. X-ray Photoelectron Spectroscopy (XPS)

X-ray Photoelectron Spectroscopy (XPS) analysis of the silica nanoparticles was performed using a Perkin Elmer Phi 5400 ESCA system X-ray photoelectron spectrometer that was operated in the Fixed Transmission Mode at constant pass energy of 187.85 eV for survey scans and 29.35 eV for higher resolution regional scans. Samples were analyzed at a take-off angle of 45° and at a base pressure of less than 10^{-8} Torr. Instrumental sensitivity factors were taken as C(1s):O(1s):N(1s):Si(2p) equals 1.000:2.330:1.580:1.170.

2.3.2. Thermogravimetric analysis (TGA)

A Q500 TA instruments thermogravimetric analyzer was used. The analysis was carried out between room temperature and 800 ºC in air with a heating rate of 10 ºC.min^{-1}.

2.3.3. Determination of APTES-SiO_2 particles content on CFs

The relative weight content of the APTES-SiO_2/epoxy coating on coated CFs, designated as $C_{s/e}$ (%), was evaluated by weighing method using Equation (1). Five samples were tested for each system.

$$C_{s/e} = \frac{W_{s/e} - W_0}{W_{s/e}} * 100 \quad (1)$$

where $W_{s/e}$ is the linear weight of CFs after dip-coating, and W_0 is the linear weight of CFs before dip-coating.

Then the relative weight content of SiO_2 particles C_s (%) on coated CFs was calculated by Equation (2):

$$C_s = C_{s/e} - C_e \quad (2)$$

where C_e is relative weight content of epoxy and APTES on CFs, which was measured by TGA following the procedure reported in section 2.3.2.

2.3.4. Observation of the surface structure of APTES-SiO_2 coated CFs by scanning electron microscopy

The uniformity and the quality of the APTES-SiO_2 coating in terms of the particle dispersion was characterized by scanning electron microscopy (SEM) with a Carl Zeiss Auriga Cross Beam field-emission scanning electron microscope. The accelerating voltage was 2 kV. The samples were coated with 3 nm of tungsten using a Leica EM MED020 modular high vacuum coating system and fixed on the sample holder with carbon tape.

2.3.5. Elemental analysis of the APTES-SiO_2 coating by energy dispersive X-ray spectroscopy

Energy dispersive X-ray spectroscopy (EDS) of the fiber surface was dome with the Carl Zeiss Carl Zeiss EVO LS25.

2.3.6. Characterization of the adhesion strength between APTES-SiO_2 coated CFs and the

epoxy matrix

Single fiber fragmentation test (SFFT) was used to measure the interfacial shear strength (IFSS) of each coated CF-epoxy matrix system[32]. The test samples were subjected to a gradual tensile load, which led to the breakage of the fiber into fragments. The tension load was increased until the number of fragments reached a maximal value (saturation state). An Olympus optical microscope with polarized light was used to determine the number of fragments and the length of each fragment. The interfacial shear strength (IFSS) was calculated with the Kelly-Tyson model[33] (Equation (3)):

$$\text{IFSS} = \frac{\sigma_f}{2}\frac{d}{l_c} \quad (3)$$

where σ_f is the fiber tensile strength corresponding to a fiber length equal to the critical fragmentation lengthl_c, d is the fiber diameter (μm) and l_c is the critical fragmentation length (μm), which can be calculated with Equation (4):

$$l_c = \frac{4}{3}\bar{l} \quad (4)$$

where $\bar{l}$ is the mean fiber fragmentation length (μm) when the saturation sate has been reached.

An Olympus optical microscope with polarized light was used to observe the photoelastic birefringence patterns generated around a fiber break when the number of fiber fragments reached saturation. This observation can give valuable information regarding the failure mode and the stress state around the breaks.

3. Results and discussion

3.1. Grafting of APTES on silica nanoparticles

The XPS analysis of the pristine silica nanoparticles and the APTES treated particles confirmed the grafting of APTES, as 2 % in nitrogen were detected in the treated particles (and no nitrogen peak was found with the pristine particles, Table 1 and Figure 2). The fitting of the N(1s) peak was done

according to component peaks suggested by Xu *et al.* [34]and by previous work[35]. The fitting showed that the amine-based groups detected at the surface of the SiO_2 particles were roughly divided in three groups with equivalent surface densities: free amines, amines involved in a hydrogen bond with the hydroxyl groups located at the surface of the particles, and protonated amines (Figure 2). The grafting of APTES was also confirmed by a dramatic increase in the carbon content (from 12 % which corresponded to a usual contamination to 40 % with the treated particles). A mechanism for the grafting of APTES on silica nano-particles is suggested in Figure 3. The ethanol that was used as the solvent was not dried. Therefore, traces of water could have reacted with APTES as well to generate bridges between grafted chains of APTES.

APTES was used to generate covalent bonding between the silica particles and the surrounding epoxy monomers by reaction of the free amine groups with the epoxide groups. A TGA analysis of the pristine silica nanoparticles (Figure 4) showed that adsorbed an amount of moisture up to 3 wt. %. This is because of their polar surface. The amount of APTES that was grafted at the surface of the particles represented a weight of 7 wt. % (Table 2).

3.2. Determination of the relative weight content in silica particles

$C_{s/e}$ and C_e of different APTES-SiO_2 coated CFs are displayed in Table 3. It was assumed that C_e was same for the different APTES-SiO_2 coated CFs and epoxy only coated CFs (APTES only represented up to 0.3 wt. % of the total weight calculated from the weight content of APTES-SiO_2 on CF and APTES content on APTES-SiO_2, which explains why no big difference was seen between samples even if the concentration in SiO_2 particles varied). C_e was calculated from the weight loss of epoxy coated CFs in step of 150 ºC to 570 ºC. The adding of SiO_2 particles in the coating solution did not affect the deposition mechanism of the epoxy monomers on the CF surface. The TGA

analysis corresponding to two different samples of APTES-SiO_2 coated CFs with a 1.3 wt. % content in silica nanoparticles were superimposable (Figure 5), which demonstrated the robustness of the process. As expected the relative weight content of SiO_2 particles increased gradually with an increase of the concentration in APTES-SiO_2 particles in the coating suspension (Table 3). The relative weight content of SiO_2 particles on CFs showed a sharp increase when the concentration of particles in the coating solution increased from 2 wt. % to 3 wt. % (Table 3). As shown, hereafter, this is related to the fact that the particles formed agglomerates at the surface of CFs when the concentration of particles in the coating solution was 3 wt. %. It is interesting to observe that CFs have slightly better thermal stability after appropriate coating as shown by the TGA curves (Figure 5a). Because the method used in this study measures the content of SiO2 particles (and not APTES-SiO2 particles), the particle concentrations reported hereafter will be referenced to SiO2 particles. Pristine silica particles were not used as reinforcement, only APTES-SiO2 particles were used for composite manufacturing.

3.3. Characterization of the surface of APTES-SiO_2 coated CFs

The energy dispersive X-ray spectroscopy (EDS) analysis of the APTES-SiO_2 coated CFs confirmed the presence of silicon (Figure 6), which did not appear in the epoxy only coated CFs. This indicates that SiO_2 nanoparticles were successfully deposited on CFs surface.

The quality of the coating on the CFs surface, in terms of homogeneity and the level of dispersion of the particles, was characterized by SEM. The surface topography of non-coated CFs was made of continuous grooves and ridges along the fiber axis (Figure 7). This topography is very typical of PAN-based carbon fibers and is produced during the spinning of the PAN precursor. The topography of the epoxy-only coated fibers was similar (Figure 7). The structure of the different

APTES-SiO_2-epoxy coatings was observed at different magnifications (Figure 8). A clear change in the surface morphologies was observed with different APTES-SiO_2 particle concentrations. A reasonably well dispersed and uniform deposition of APTES-SiO_2 particles on the CF surfaces is achieved at low concentrations (such as 1.0 wt. % and 1.3 wt. %) (Figures 8a and 8b). At higher concentrations (i.e. 1.7 wt. %, 3.4 wt. %), agglomerates of APTES-SiO_2 particles are formed (Figures 8c and 8d). It is obvious that the aggregation is severe with a concentration in SiO_2 particles of 3.4 wt. %. The thickness of APTES-SiO_2-epoxy coatings was between 0.2 and 1.1 μm, based on the difference in diameter (measured with SEM images) between non-coated and coated CFs. The diameter of non-coated CFs was indeed 7.1 μm and the diameter of APTES-SiO_2 coated CFS was between 7.3 and 8.2 μm. It is expected that the quality of the dispersion and the concentration of silica nanoparticles will have a direct influence on the level of adhesion strength between the CFs and the epoxy matrix.

3.4. Influence of APTES-SiO_2 coating on adhesion strength between the CFs and the epoxy matrix

To better understand the relationship between the properties of the APTES-SiO_2 coatings and the mechanical properties in the interphase region, a single fiber fragmentation test was employed to measure the interfacial shear strength (IFSS) of the CF/epoxy matrix interface. The IFSS evaluates the level of interfacial adhesion between the carbon fiber surface and the epoxy matrix and is a function of the fiber surface properties and the mechanical properties of the coating (if any). The typical distribution of the fiber fragments length at the saturation state is shown in Figure 9 for each CF-epoxy system. It is clear that a shift towards shorter fragments length was associated to APTES-SiO_2 coated CFs with concentrations in SiO_2 particles of 1.0 wt. % and 1.3 wt. % and with

epoxy-only coated CFs as well. A concentration in SiO_2 particles of 1 wt. % resulted in the shortest fragments lengths. Only APTES-SiO_2 coated CFs with concentrations in SiO_2 particles of 3.4 wt. % showed fragments length that were overall longer in comparison to non-coated CFs.

The IFSS corresponding to each system is tabulated in Table 4. Since all fibers were surface treated with the same UV/ozone oxidation surface treatment, the level of interactions between the CFs surface and the epoxy coating were the same. The observed increase in the IFSS is the result of more efficient stress transfer from the matrix to the fiber surface in the interphase region as a result of the incorporation of the APTES-SiO2 particles. A very slight increase was noticed for epoxy-only coated CFs. The initial epoxy coating has a lower concentration of curing agent than the bulk matrix. Diffusion coupled with reaction of the curing agent into the epoxy coating produces a gradient in curing agent from the matrix to the fiber surface. Drzal *et al.*[18], have shown that a stiffer interphase with a higher shear modulus compared to the bulk of the matrix is formed, which improves the stress transfer from the matrix to the fiber surface as postulated by Cox's shear-lag analysis[36] for example.

The IFSS of APTES-SiO_2 coated CFs have a higher IFSS compared to non-coated CFs and epoxy-only coated CFs. The maximum value was obtained for a concentration in SiO_2 particles of 1.3 wt. % and represented an increase of 44 % and 33 % compared to non-coated CFs and epoxy-only coated CFs, respectively. Because of the incorporation of the silica-nanoparticles in the interphase region, the shear modulus of the matrix in the interphase region is higher in comparison to the bulk (and is higher compared to shear modulus of the interphase generated by an epoxy-only coating). Shear lag analysis explains the higher IFSS as a result of the increase in the interphase shear modulus. In addition, the presence of APTES-SiO_2 nanoparticles in the interphase provides a

crack deflection mechanism and possibly cavitation at the interface[37]due to the particle debonding[38].

When the concentration of APTES-SiO_2 particles is too high, large agglomerates are produced as shown with a concentration in SiO_2 particles of 3.4 wt. % (Figure 8d). The SiO2 agglomerates act as stress concentrators, decreasing the strength of the interphase region. This results in longer fragments lengths when the saturation state is reached during the single fiber fragmentation test (Table 4), and to lower values of the IFSS (Table 4).

Overall, higher values of IFSS can be attained by incorporating silica nanoparticles in the interphase region through a fiber coating process, but only if the dispersion of those particles is optimal in terms of concentration, homogeneity, and separation of individual particles.

3.5. Observation of the birefringence patterns generated during the single fiber fragmentation test

This birefringence patterns observed under transmitted polarized light during the single fiber fragmentation test indicate the level of local shear stress in the interphase[39]. The shear stress is distributed near a fiber break, or near the ends of a fragment. Stress located at the interface can lead to interfacial debonding between the fiber surface and the matrix or cohesive failure in the interphase. The local shear stress decreases as there is debonding or damage close to the fiber/matrix interface. The stress birefringence patterns become longer and flatter and the local maximum intensity can shift away from the fragment ends. The birefringence patterns obtained for the different CF-epoxy composites at the saturation state are shown in Figure 10. The level of stress generated locally close to the breaks differed strongly, as well as the fracture patterns. Non-coated CFs produce a weak diffuse birefringence pattern around the fiber breaks, which corresponds to poor/moderate interfacial bonding. The patterns became more intense with an epoxy coating but the local maximum stress was

located away from the fragment ends.

A concentration in SiO_2 nanoparticles of 1.3 wt. % resulted in more intense birefringence patterns located closer to the fiber breaks. This agrees with the interpretation that a reinforced interphase results in more efficient stress transfer. For a concentration in SiO_2 particles of 3.4 wt. %, the birefringence patterns were dull, just like in the case of non-coated fibers. This is the result of an interphase that is very thick and weak from a very high concentration of particles. Overall, the birefringence patterns were consistent with the IFSS values.

4. Conclusions

APTES-SiO_2 nanoparticles coated CFs were fabricated using a simple dipping method. CFs fibers were immersed for few seconds in a silica nanoparticle suspension. The influence of the nanoparticles concentration in the coating suspension on the quality of the coating (homogeneity, quality of the dispersion of the particles) was investigated. An optimal concentration was found which produced a large density of particles at the CFs surface without significant aggregation. The influence of the coating structure (concentration of silica particles, dispersion of the particles, homogeneity) on the mechanical properties in the interphase region was investigated using the single fiber fragmentation test. Uniform coating with well dispersed particles led to an increase of the IFSS because of an increase of the shear modulus of the interphase region. An increase in IFSS of 44 % and 34 % was measured compared with non-coated CFs and epoxy-only coated fibers, respectively. On the contrary, when the concentration in silica nanoparticles was too high and aggregates were formed, the IFSS was low, even lower in comparison to non-coated fibers. Those aggregates represented defects in the coating structure and affected the stress transfer from the matrix to the fiber surface. All in all, it was shown that a very simple process consisting of coating silica

nanoparticles onto CFs could lead to a significant improvement of the adhesion strength of the interface and consequently to a potential improvement of the mechanical properties of the corresponding composites. The process can be easily scaled-up and integrated into a CF production line.

Acknowledgment

This work was financially supported by the China Scholarship Council and Composite Materials and Structures Center, Michigan State University (RC103337). The authors appreciated the support of the. Hexcel Co, and Hexion for supplying CFs. Edward Drown from the Composite Materials and Structures Center of Michigan State University is acknowledged for his contribution in the production of UV/ozone surface treated CFs. Many thanks to Michael Rich and Brian Rook from the Composite Materials and Structures Center for their training, collaboration and advice.

References:

1. B. Jahn and E. Witten.E, Composites Market Report ,2013.
2. L.T. Drzal and M. Madukar, *J. Mater .Sci.*, 1993, **28**, 569-610.
3. F. Vautard, P. Fioux, L. Vidal, J. Schultz, M. Nardin and B. Defoort, *Compos. Part .A.*, 2011, **42**, 859-867.
4. X.Q.Zhang, H.B. Xu and X. Y. Fan, *RSC. Adv.*, 2014, **4**, 12198-12205.
5. L. T. Drzal, *Mater. Sci.Eng A.*, 1990, **126**, 289-293.
6. L. C. Ma, L. H. Meng, Y.W. Wang, G.S. Wu, D.P. Fan, J.L. Yu,M.W. Qi and Y. D. Huang, *RSC. Adv.*, 2014, **4**, 39156-39166.
7. F. Vautard, H. Grappe and S. Ozcan, *Ind.Eng. Chem. Res*., 2014, **53**, 12729-12736.
8. L.T.Drzal, M.Madhukar and M.C. Waterbury, *Compos.Struct.*, 1994, **27**, 65-71.
9. F. Vautard, P. Fioux, L. Vidal, J. Dentzer, J. Schultz, M. Nardin and B. Defoort, *Surf.Interface. Anal.*, 2013, **45**, 722-741.
10. F. Vautard, S. Ozcan and H. Meyer, *Compos. Part A.,* 2012, **43**, 1120-1133.
11. L. T. Drzal, M. J. Rich, B. P. Rook, P. Askeland and E. K. Drown, *Proceedings of the 17th International Conference on Composite Materials, Edinburgh, Scotland,* 2009.
12. R.X. Gu, J.R. Yu, C.C. Hu, L. Chen, J. Zhu and Z.M. Hu, *Appl. Surf. Sci.*, 2012, **258**, 10168-10174.
13. F. Vautard, P. Fioux, L. Vidal, J. Dentzer, J. Schultz, M. Nardin and B. Defoort, *J. Adhes.*, 2013, **89**, 460-485.
14. Z. Liu, C. Tang, P. Chen, Q. Yu and W.K. Li, *RSC. Adv*, 2014, **4**, 26881-26887.
15. F. Vautard, P. Fioux, L. c. Vidal, F. Siffer, V. Roucoules, J. Schultz, M. Nardin and B. Defoort, *ACS. Appl. Mater. Interfaces.*, 2014, **6**, 1662-1667.
16. L. T. Drzal, N. Sugiura and D. Hook, *Compos. Interfaces.*, 1997, **4**, 337-354.

17. A.Paipetis and C. Galiotis, *Compos.Part A*., 1996, **27**, 755-767.
18. L. T. Drzal, M. J. Rich, M. F. Koenig and P. F. Lloyd, *J. Adhes.*, 1983, **16**, 133-152.
19. T.H.Cheng, J.Zhang, S. Yumitori and F.R Jones., *Composite.*, 1994, **25**, 661-670.
20. S. K. Kumar and R. Krishnamoorti, *Annu.Revi.Chem. Biomol. Eng.*, 2010, **1**, 37-58.
21. T. Kamae and L. T. Drzal, *Compos. Part A.,* 2012, **43**, 1569-1577.
22. J. K. Park, I-H. Do, P. Askeland and L. T. Drzal, *Compos. Sci. Technol.*, 2008, **68**, 1734-1741.
23. W. Lee, J. UK. Lee, H-J. Cha and J-H. Byun, *RSC. Adv.*, 2013, **3**, 25609-25613.
24. Y. G. Niu, X. Zhang, W.Z. Pan, J.P. Zhao and Y. Li, *RSC. Adv.*, 2014, **4**, 7511-7515.
25. J. Qian,J.L. Wu, X.Y.Liu, Q. X.Zhuang and Z. W. Han , *J. Appl. Poly. Sci.*, 2013, **127**, 2990-2995.
26. Y. L. Liu and S.H. Li, *J. Appl. Poly. Sci.* 2005, **95**, 1237-1245.
27. L.X. Yuan, H.X. Yan, Y. Jia and T. T. Li, *J.Reinf. Plas. Compos.*, 2014, **33**, 1743-1750.
28. H. Nabeshi, T. Yoshikawa, A. Arimori, T. Yoshida, T. Saeko, T. Hirai,T. Akase, K. Nagano, Y. Abe, H. Kamada, S.I. Tsunoda, N. Itoh,Y. Yoshioka and Y. Tsutsumi, *Nanoscale. Res. Lett.*, 2011,**6**, 93
29. L. Liu, L. Li, Y. Gao, L.C. Tang and Z. Zhang, *Compos. Sc i. Technol.*, 2013, **77**, 101-109.
30. T. H. Hsieh, A. J. Kinloch, K. Masania, J. Sohn Lee, A. C. Taylor and S. Sprenger, *J.Mater. Sci.*, 2009, **45**, 1193-1210.
31. L.T. Drzal and M.J.Rich, US *Pat.,*6, *649 225*, 2003.
32. P.J.Herrera-Franco and L.T. Drzal, *Composite*, 1992, **23**, 1-27.
33. A. Kelly and W.R. Tyson, *J. Mech. Phys.Solids*, 1965, **13**, 329-338.
34. Z. H.Xu, Q. X.Liu and J.A.Finch , *Appl. Surf. Sci.*, 1997, **120**, 269-278.
35. F. Vautard, H. Grappe and S. Ozcan, *Appl. Surf. Sci.*, 2013, **268**, 61-72.
36. H.L. Cox, *Br. J. Appl. Phy.,* 1952, **3**, 72-79.
37. Y. Zheng, *J.Reinf. Plas. Compos.*, 2005, **24**, 223-233.
38. J. L. Tsai, H. Hsiao and Y. L. Cheng, *J.Compos. Mater.,* 2009, **44**, 505-524.
39. B.W.Kim and J.A. Nairn, *J .Compos. Mater.*, 2002, **36**, 1825-1858.

Table 1. Elemental analysis of pristine and functionaziled silica nanoparticles by XPS.

	C (%)	N (%)	O (%)	Si (%)
Pristine SiO_2	12	0	64	24
APTES-SiO_2	40	2	40	18

Table 2. The weight loss of pristine SiO_2, APTES-SiO_2 and APTES in different step from TGA

	Weight loss (wt.%) in RT-100 ºC	Weight loss (wt.%) in 100 ºC -650 ºC
Pristine SiO_2	2.8	1.4
APTES-SiO_2	1.5	8.2
APTES	1.2	98.8

Table 3. C_e, $C_{s/e}$ and calculated C_s for different APTES-SiO_2 coated CFs.

APTES-SiO_2 concentration in epoxy solution (wt.%)	C_e (wt. %)	$C_{s/e}$ (wt. %)	C_s (wt. %)
0	1.1 ± 0.2	-	-
0.5	1.1 ± 0.2	2.1 ± 0.1	1.0 ± 0.1
1	1.1 ± 0.2	2.4 ± 0.2	1.3 ± 0.2
2	1.1 ± 0.2	2.8 ± 0.1	1.7 ± 0.1
3	1.1 ± 0.2	4.5 ± 0.3	3.4 ± 0.3

Table 4. Interfacial shear strength of CF/epoxy systems measured by the fragmentation test.

Sample	l_c/d	IFSS (MPa)	Relative increase (%)	
			a	b
Non-coated CF	62 ± 4	36 ± 3	-	-
Epoxy-only coated	57 ± 3	39 ± 2	8	-
1.0 wt. % SiO_2	49 ± 4	45 ± 4	25	15
1.3 wt. % SiO_2	43 ± 1	52 ± 1	44	33
1.7 wt. % SiO_2	48 ± 2	46 ± 1	28	18
3.4 wt. % SiO_2	64 ± 7	35 ± 4	-3	-10

"Relative increase (%)" calculation: non-coated CF was considered as the reference material for column (a), epoxy-only coated was the reference material for column (b).

Figure Captions:

Figure 1. Schematic of the dip-coating process.

Figure 2. XPS survey spetrum and N1(s) peak corresponding to APTES-SiO_2 particles.

Figure 3. Mechanism of APTES grafting on the surface of SiO_2 nano-particles.

Figure 4. TGA analysis in air of APTES, pristine SiO_2 particles, and APTES grafted particles.

Figure 5. TGA analysis of (a) neat Epon 828, non-coated CFs, epoxy-only coated CFs, and APTES-SiO_2 coated CF_S, (b) APTES-SiO_2 coated CFs with 1.3 wt. % in SiO_2 particles and epoxy-only coated CFs.

Figure 6. EDS analysis of the surface of (a) non-coated CFs and (b) 1.3 wt. % APTES-SiO_2 coated CFs.

Figure 7. SEM observation of the surface topography of (a) non-coated CFs, (b) epoxy-only coated CFs.

Figure 8. SEM observation of APTES-SiO_2 coated CFs with different SiO_2 particle concentrations at various magnifications: (a) 1.0 wt. % SiO_2 particles, (b) 1.3 wt. % SiO_2 particles, (c) 1.7wt. % SiO_2 particles, (d) 3.4 wt. % SiO_2 particles.

Figure 9. Frequency distribution of the CF fragments length at saturation state.

Figure 10. Birefringence patterns obtained at the saturation state: (a) non-coated CFs, (b) epoxy-only coated CFs, (c) 1.0 wt. % SiO_2 coated CFs, (d) 1.3 wt. % SiO_2 coated CFs, (e) 1.7 wt. % SiO_2 coated CFs, (f) 3.4 wt. % SiO_2 coated CFs.

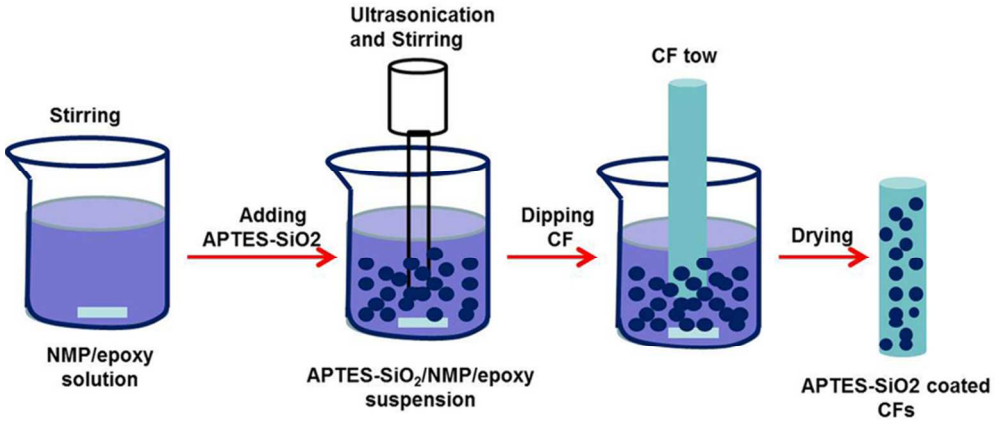

Figure 1. Schematic of the dip-coating process.
74x32mm (300 x 300 DPI)

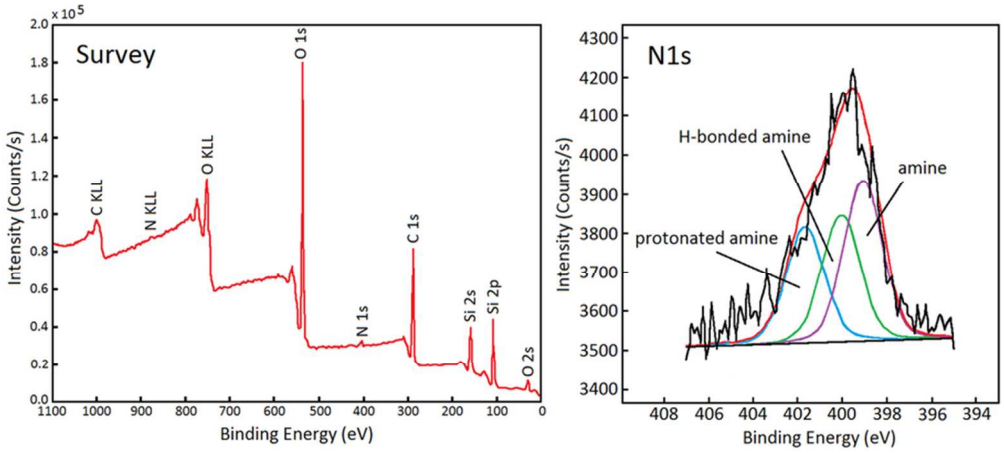

Figure 2. XPS survey spetrum and N1(s) peak corresponding to APTES-SiO2 particles.
76x34mm (300 x 300 DPI)

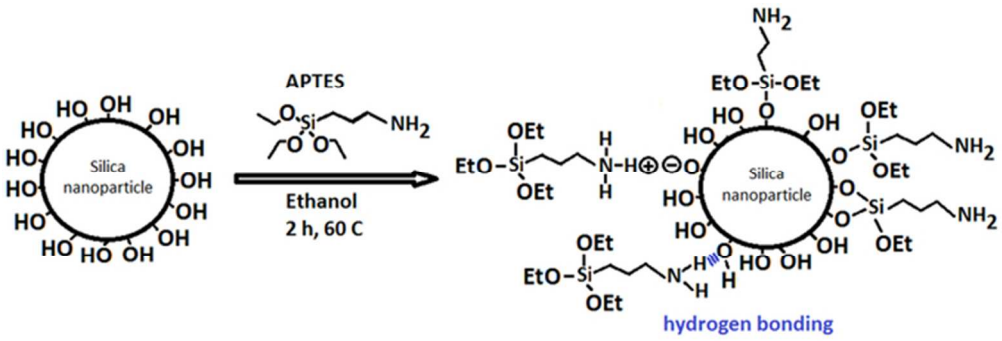

Figure 3. Mechanism of APTES grafting on the surface of SiO2 nano-particles.
57x19mm (300 x 300 DPI)

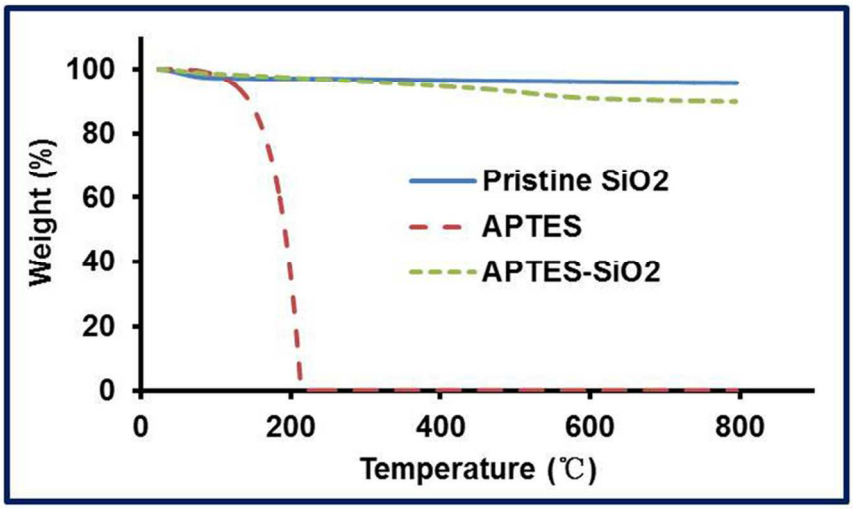

Figure 4. TGA analysis in air of APTES, pristine SiO2 particles, and APTES grafted particles.
44x24mm (600 x 600 DPI)

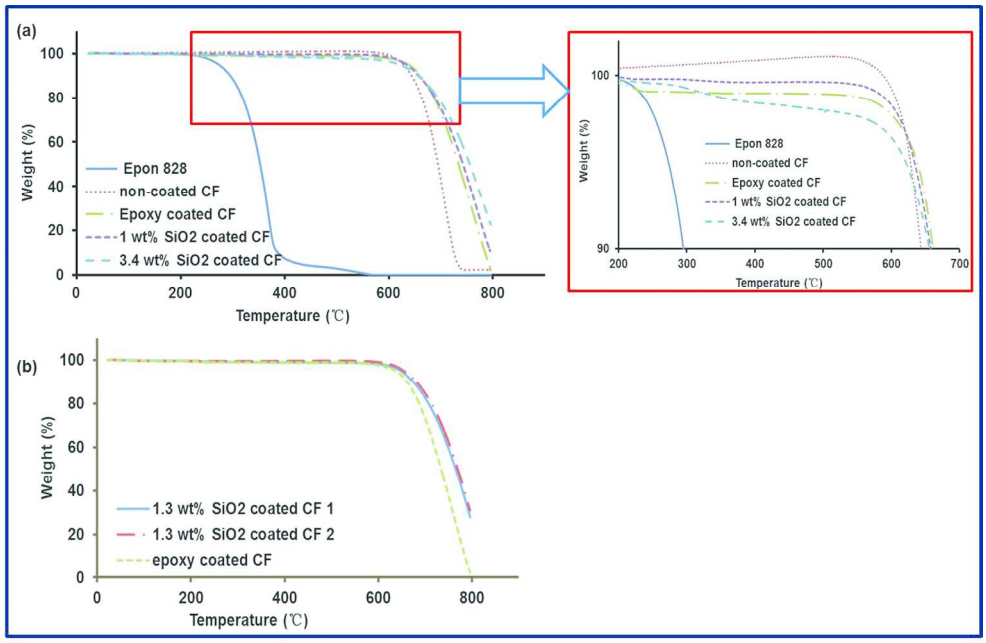

Figure 5. TGA analysis of (a) neat Epon 828, non-coated CFs, epoxy-only coated CFs, and APTES-SiO2 coated CFS, (b) APTES-SiO2 coated CFs with 1.3 wt. % in SiO2 particles and epoxy-only coated CFs.
112x73mm (600 x 600 DPI)

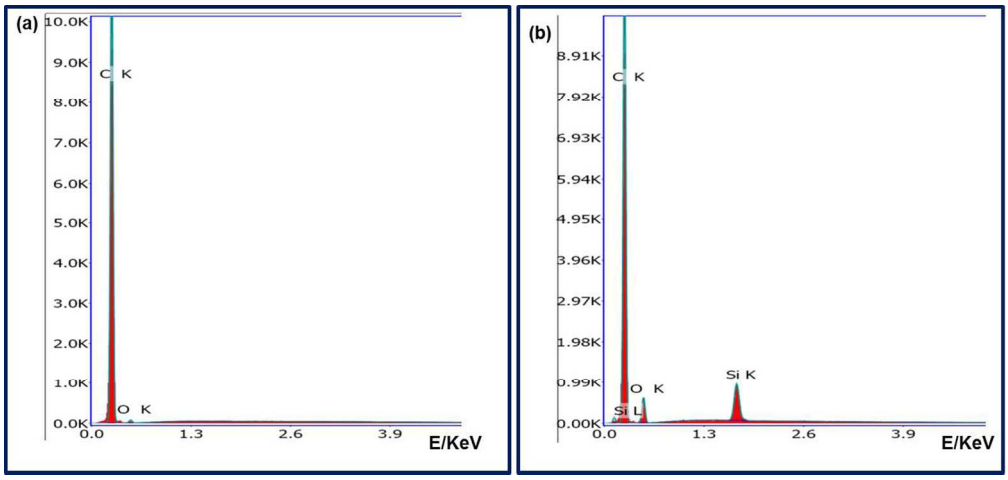

Figure 6. EDS analysis of the surface of (a) non-coated CFs and (b) 1.3 wt. % APTES-SiO2 coated CFs.
80x37mm (600 x 600 DPI)

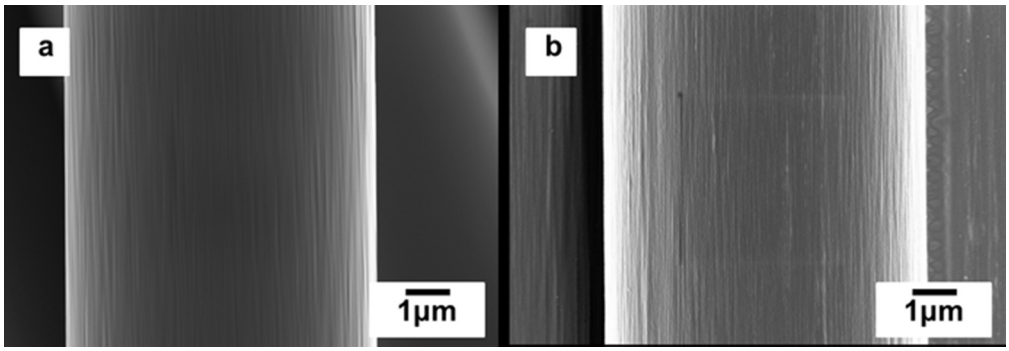

Figure 7. SEM observation of the surface topography of (a) non-coated CFs, (b) epoxy-only coated CFs
58x19mm (300 x 300 DPI)

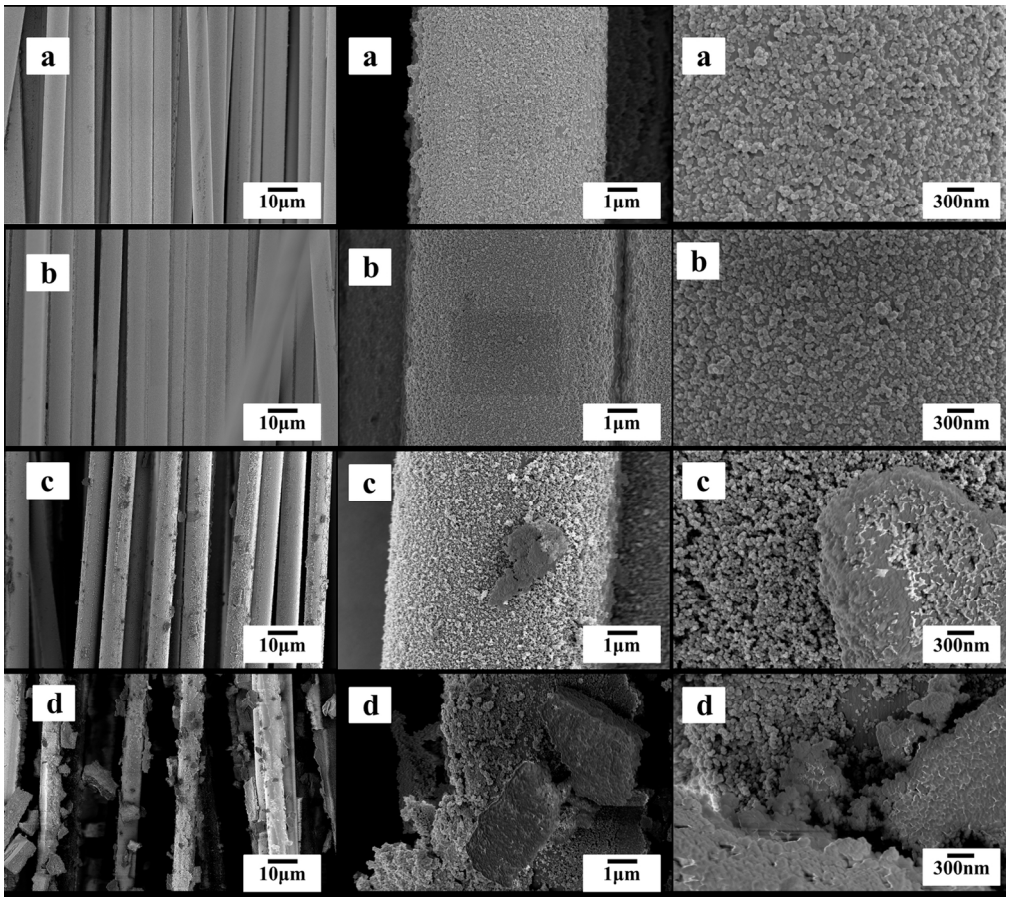

Figure 8. SEM observation of APTES-SiO2 coated CFs with different SiO2 particle concentrations at various magnifications: (a) 1.0 wt. % SiO2 particles, (b) 1.3 wt. % SiO2 particles, (c) 1.7wt. % SiO2 particles, (d) 3.4 wt. % SiO2 particles.
152x135mm (300 x 300 DPI)

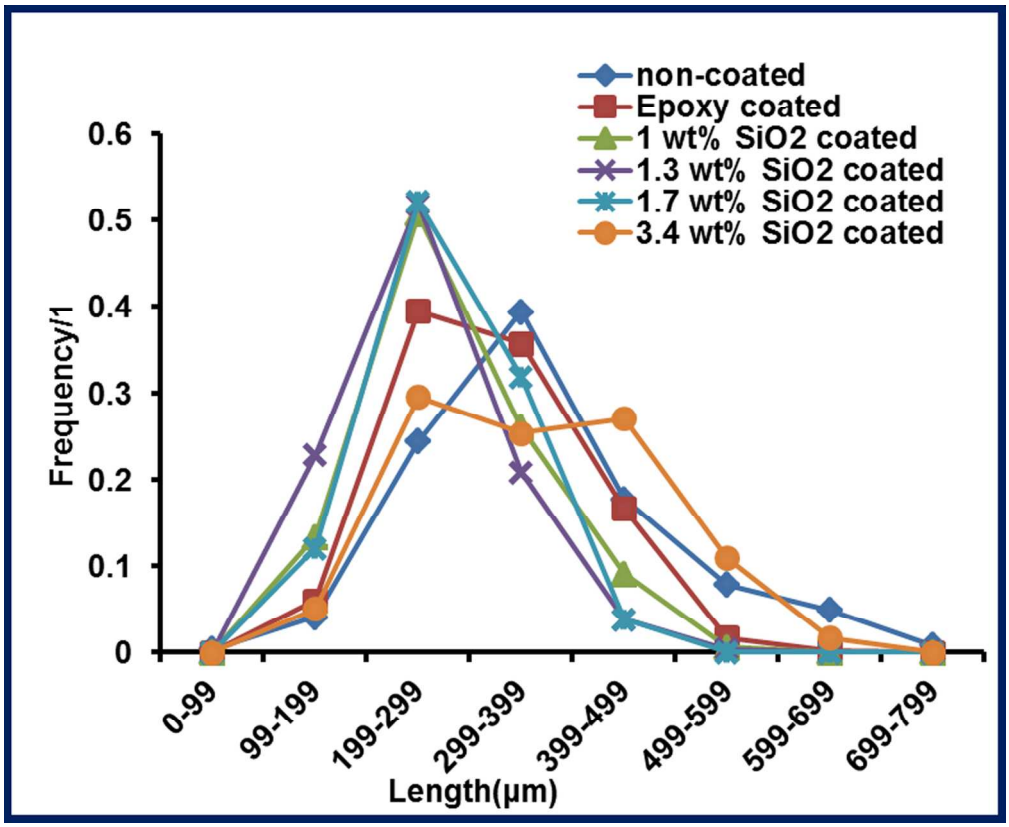

Figure 9. Frequency distribution of the CF fragments length at saturation state.
67x55mm (600 x 600 DPI)

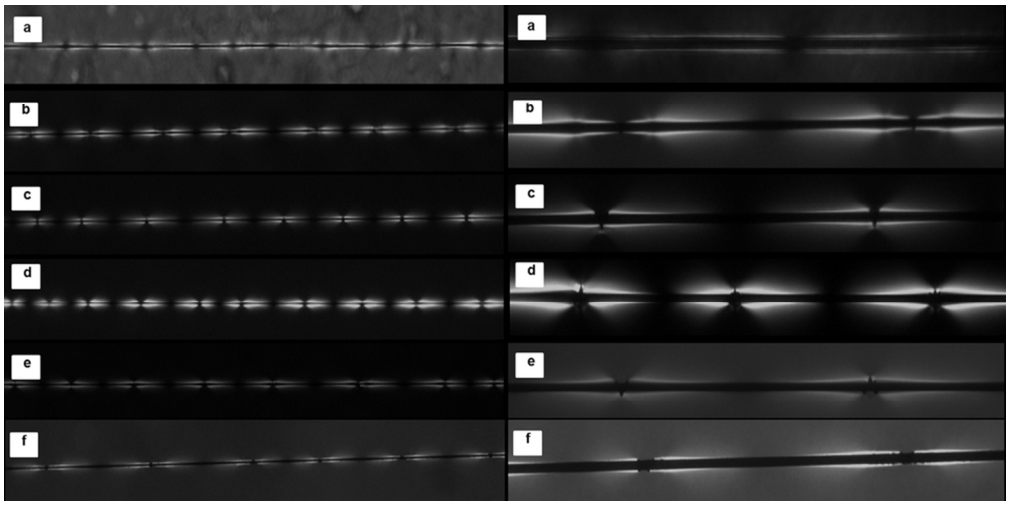

Figure 10. Birefringence patterns obtained at the saturation state: (a) non-coated CFs, (b) epoxy-only coated CFs, (c) 1.0 wt. % SiO2 coated CFs, (d) 1.3 wt. % SiO2 coated CFs, (e) 1.7 wt. % SiO2 coated CFs, (f) 3.4 wt. % SiO2 coated CFs.
84x41mm (300 x 300 DPI)

Graphical Abstract:

The carbon fiber surface was modified by Silicon dioxide nanoparticles by immersing CFs tows in a SiO_2 nanoparticle suspension. A significant increase of the IFSS was obtained.